Article

Journal of the Brazilian Chemical Society

https://dx.doi.org/10.21577/0103-5053.20240124

J. Braz. Chem. Soc. **2024**, *35*, 12, e-20240124, 1-6

Synthesis of Cadmium Oxyorthosilicate by a Sol-Gel Method

***Elena I. A. H. P. Santos*[a] *and Flavio M. Vichi*[*,a]**

[a]*Instituto de Química, Universidade de São Paulo, Av. Prof. Lineu Prestes, 748, Bloco 3T, Sala 325, 5508-900 São Paulo-SP, Brazil*

Cadmium silicates are materials of interest due to their stability and possible application as phosphors. There are three stable forms: cadmium metasilicate, $CdSiO_3$, cadmium orthosilicate, Cd_2SiO_4 and cadmium oxyorthosilicate, Cd_3SiO_5. Of these, oxyorthosilicate is particularly challenging to obtain, leading to fewer studies. We have successfully prepared Cd_3SiO_5 using a sol-gel approach, employing cadmium acetate and tetraethylorthosilicate as precursors in a stoichiometric proportion of 2:1. Additionally, cetyltrimethylammonium bromide served as a template for creating a mesoporous structure. Adjusting the pH to 3 and subjecting the material to calcination at 800 °C for 6 h, we achieved the formation of cadmium oxyorthosilicate compound, identified by X-ray diffraction. Electron diffractometry and energy dispersive X-ray spectrometry confirm the phase purity. Characterization via nitrogen adsorption analysis and transmission microscopy shows aggregates of nanoparticles with a surface area of 6 $m^2\ g^{-1}$ and a narrow pore diameter distribution centered at 5 nm.

Keywords: sol-gel, cadmium oxyorthosilicate, mesoporous, phosphor matrix

Introduction

Cadmium silicates are materials of interest due to their stability under moisture and acidic conditions. A possibility of tailoring phosphors exists in this matrix, due to the ionic radius similarity between Cd^{2+} and the most common doping agents, rare earth ions, and to the ionic nature of the Cd bonds in the structure.[1,2]

Specifically, cadmium metasilicate ($CdSiO_3$) features intrinsic persistent luminescence,[3] and therefore dispenses the need of an activator or a sensitizer for luminescence to occur.[4] Materials with persistent luminescence can be and are used in several fields, such as security lighting, toys, light emitting diodes (LEDs) as well as bioimaging and fingerprint identification.[4,5]

Silicate synthesis is also being studied as a metal stabilization technique for heavy metal removal.[6] Cadmium is widely applied in alkaline batteries and metallurgical alloying due to its chemical properties. It is also naturally found as a component in some coals.[7] These applications and its incineration as a solid waste have led to environmental contamination.[7,8] Although cadmium and its oxides are very toxic, it has been shown that, when ionically bound to silicates, ion exchange does not occur at ambient conditions and therefore no cadmium is released into the environment.[9]

Stable cadmium silicate forms in three distinct phases: metasilicate-monoclinic $CdSiO_3$ space group P21/c similar to parawollastonita;[1,10,11] orthosilicate-orthorhombic Cd_2SiO_4 similar to thernadite, Na_2SiO_4;[1,11] and oxyorthosilicate-tetragonal Cd_3SiO_5 of the space group P4/nmm.[12]

The structure of Cd_3SiO_5 is comprised of two non-equivalent Cd^{2+} sites: one with Cd penta-coordinated with five O^{2-}, where one Cd–O bond is shorter (217 pm) than the others (231 pm); and a second site where Cd is in distorted CdO_6 octahedra surrounding SiO_4 tetrahedra.[12] The structure of Cd_3SiO_5 has also been described as pseudo-rhombohedral due to similarities with the structure of Ca_3SiO_5, but with a resemblance to the tetragonal structure of Sr_3SiO_5.[1,13] Cadmium oxide-orthosilicate structure differs

*e-mail: fmvichi@iq.usp.br
Editor handled this article: Aldo José Gorgatti Zarbin (Guest)
A tribute to Prof Oswaldo Luiz Alves. "Oswaldo was not only a great and inspiring scientist. He also knew the importance of happiness and fulfillment. – Go to a movie, to a concert! – he would say. Of his many advices, I consider this to be the most important: Enjoy the ride of learning and discovery, but never get so caught up in it that you don't look around yourself. Look sideways to your colleagues and relatives, look up to those more experienced and wiser, and never, never forget to look down to those who are less fortunate, those who depend the most on the advancement of science."

from the other cadmium silicates because of the presence of Cd–O–Cd bonds.[14]

The metasilicate, $CdSiO_3$, has been extensively studied as a phosphor. It is normally obtained by solid state reaction at temperatures above 1050 °C, but it can be easily obtained at temperatures as low as 580 °C using a molten precursor approach, as we have previously reported.[15] The pure solid exhibits emission when excited at 240 nm, a wavelength close to the reported band-gap energy (5.18 eV).[16] Emission occurs mainly in three wavelengths: 590, 490 and 406 nm.[17] The synthetic method is known to affect the intensity and the presence or absence of certain emissions as a consequence of defects created in the matrix.[18]

Studies have also been conducted with the orthosilicate, Cd_2SiO_4, which has a smaller band gap than $CdSiO_3$.[1] It does not display intrinsic luminescence, and therefore requires some sort of activator.[4] For instance, doping with Pr^{III} results in a persistent phosphor, while doping with Tb^{III} does not.[11] The luminescence mechanism is also being studied for these different phosphors.[11,19]

Cadmium oxyorthosilicate, Cd_3SiO_5, however, has not received as much attention due to difficulty in obtaining it as a single, or even major phase. It has been reported as an unwanted minor phase, generally in combination with one or both of the other phases.[1,6,11] In this paper we present a method for the synthesis of the oxyorthosilicate using a sol-gel method. To the best of our knowledge, this is the first report of the preparation of this material as a single phase.

Experimental

The reagents used were: cadmium acetate $CdC_4H_6O_4.2H_2O$ (99%, Sigma-Aldrich, Milwaukee, USA), tetraethylorthosilicate (TEOS) (98%, Sigma-Aldrich, Milwaukee, USA) cetyltrimethylammonium bromide (CTAB) (98%, Sigma-Aldrich, Milwaukee, USA), hydrochloric acid HCl (Merck, São Paulo, Brazil) and sodium hydroxide NaOH (Merck, São Paulo, Brazil). All were commercially available and employed without further purification.

The sol-gel method was applied as follows: 0.6 g of CTAB (0.0016 mol) were dissolved in 288 mL of deionized water. Next, 3.36 g (0.0126 mol) of $CdC_4H_6O_4.2H_2O$ were added to this solution, followed by dropwise addition of 1.3 mL (0.006 mol) of tetraethylorthosilicate, corresponding to a Cd/Si molar ratio of 2. The system was kept under constant stirring for 2 h at 80 °C. The pH was controlled using small amounts of HCl or NaOH adjusting to pH values of 3, 5, 7 and 8. Transparent, clear sols were observed in acidic and neutral solutions while a translucent milk-like sol was obtained for pH 8. The sols were dried at 70 °C for 96 h, resulting in dried gels that were calcined at 600 or 800 °C for 6 h.

X-ray powder diffractometry (XRD) patterns were obtained for all samples using a Shimadzu Maxima XRD-7000 (Tokyo, Japan) diffractometer, Cu Kα radiation (0.15418 nm), at a scan rate of 2° *per* min. The diffraction data were collected from the angles $2\theta = 10$ to 60°. All results were compared to the JCPDS (Joint Committee on Powder Diffraction Standards) database library.

Transmission electron microscopy (TEM) images were acquired using a JEOL JEM 2100 microscope (Tokyo, Japan) with an accelerating voltage of 200 kV. Energy dispersive X-ray spectrometry (EDS) was performed as well as selected area electron diffraction (SAED) to confirm sample purity. SAED image was captured using a charge-coupled device (CCD).

Surface area and pore diameter distribution were calculated by the Brunauer-Emmett-Teller (BET) method using N_2 adsorption/desorption isotherms obtained with a Quantachrome Nova 1000e equipment (Belvidere, IL, USA). The samples were purged under static vacuum at 300 °C for 10 h prior to analysis.

Results and Discussion

Calcination temperature was studied by applying two different temperatures: 600 and 800 °C. The XRD pattern (Figure 1) shows that calcination at 600 °C was not sufficient to obtain the desired phase, as exemplified in Figure 1 for pH 5 and 8. Some peaks indicate cadmium oxide and silica formation as well as the silicates Cd_2SiO_4 and Cd_3SiO_5. Using pH 8 (Figure 1a) resulted in a more pronounced amorphous silica halo at $25° < 2\theta < 35°$ than the sample formed using pH 5 (Figure 1b).

Samples calcinated at 800 °C (Figure 2), however, displays formation of identifiable cadmium silicate phases. Different pH conditions were also used during the sol-gel synthesis. Diffraction patterns can be associated to the phases Cd_2SiO_4 and Cd_3SiO_5.

It can be seen that, while Cd_2SiO_4 is formed under less acidic conditions (Figure 2a), the desired Cd_3SiO_5 phase is favored as the acidity increases (Figure 2d). Moreover, the samples become more crystalline at lower pH, as shown by their more intense peaks. This tendency of "contamination with Cd_3SiO_5" under more acidic conditions is observed for orthosilicate in other studies,[18,20] and could be associated with some factors in the sol-gel synthesis: speed of gel formation and hydrolysis, as well as cadmium availability. The sol-gel method is greatly influenced by pH.[21] It occurs in two processes: hydrolysis and condensation. While

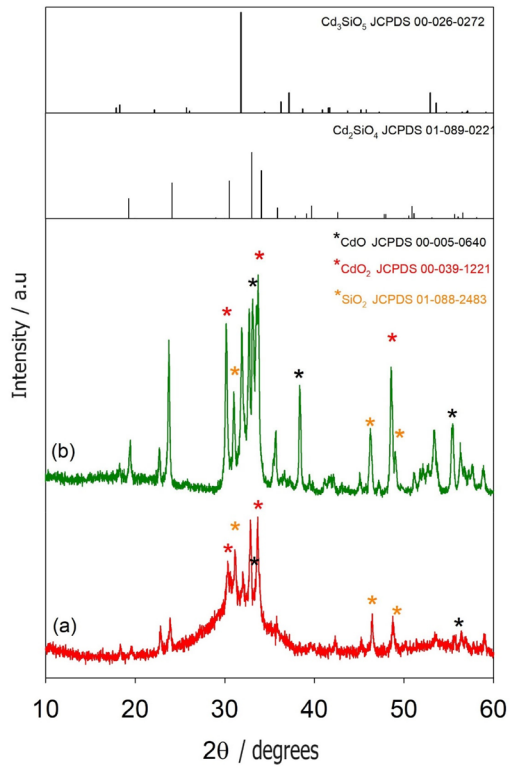

Figure 1. XRD patterns of samples obtained at 600 °C prepared at (a) pH 8 (sample 1) and (b) pH 5 (sample 2) with the JCPDS No. 01-089-0221 Cd_2SiO_4 and JCPDS No. 00-026-0272 Cd_3SiO_5 cards for comparison.

hydrolysis is favored in an acidic medium, the condensation process is accelerated under basic conditions, which interferes in the interaction between cadmium and silica network.[21,22]

Under alkaline conditions, there is also a competition between the formation of cadmium hydroxide and the silicate precursor. Hydroxide can then decompose into CdO during calcination, as shown in equation 1.[20,23]

$$Cd^{2+} + OH^- \rightarrow Cd(OH)_2 \rightarrow CdO \quad (1)$$

This oxide can react with SiO_2 resulting in one of the cadmium silicate phases, or mixtures of them (equations 2, 3 and 4). The details of these mechanisms are currently under study, but experimental data suggest the following reactions for the formation of these species:[6,24-27]

$$CdO + SiO_2 \rightarrow CdSiO_3 \quad (2)$$
$$2CdO + SiO_2 \rightarrow Cd_2SiO_4 \quad (3)$$
$$3CdO + SiO_2 \rightarrow Cd_3SiO_5 \quad (4)$$

There is also the possibility of conversion between phases (equation 5):

$$Cd_2SiO_4 + CdO \rightleftarrows Cd_3SiO_5 \quad (5)$$

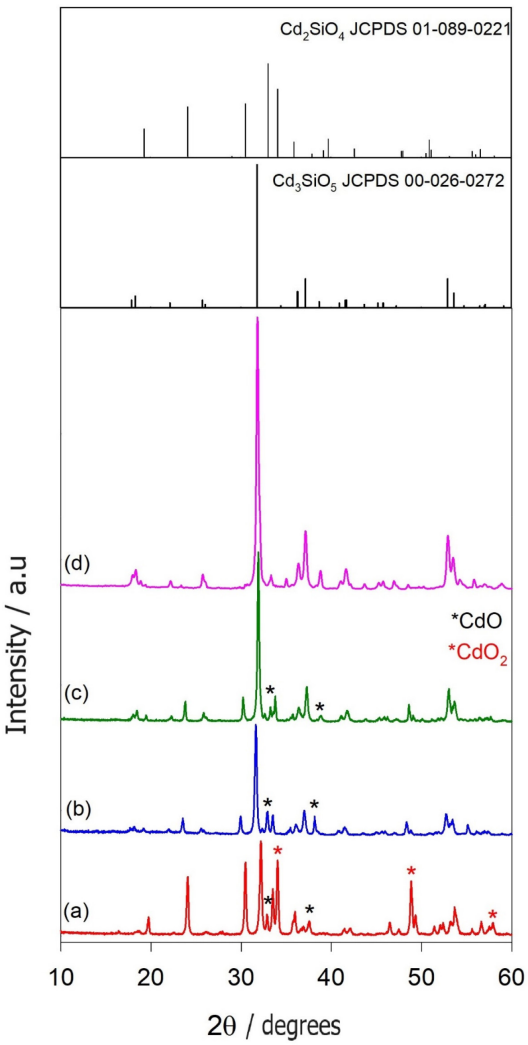

Figure 2. XDR patterns samples obtained at 800 °C prepared at (a) pH 8 (sample 3), (b) pH 7 (sample 4), (c) pH 5 (sample 5), and (d) pH 3 (sample 6) with JCPDS No. 01-089-0221 Cd_2SiO_4 and JCPDS No. 00-026-0272 Cd_3SiO_5 cards for comparison.

And so, while the excess of CdO forms preferably Cd_3SiO_5, its volatility and its consumption during the reaction shifts the process towards the formation of Cd_2SiO_4.[28,29]

The crystallite size of samples 4, 5, and 6 were estimated using the Scherrer equation (Table 1). For Cd_3SiO_5, the peak at 31.8° exhibits highest intensity and therefore was used for calculation.

From Table 1 it is possible to notice a shift in the position of the diffraction peak ranging from 31.6 to 31.9°. This difference is normally associated with lattice distortion and defects. Sample 6 resulted in the closest structure and a crystallite size of 24 nm.

TEM images were obtained for sample 6, corresponding to single-phase Cd_3SiO_5. The images show the presence of aggregates (Figure 3a) ranging from 500 to 3000 nm. Figure 3b highlights the coalescence of these particles.

Table 1. Crystallite size calculated by Scherrer equation

Sample name	Crystallite size calculated / nm	Peak position (2θ)[a] / degree
Sample 4	25	31.6
Sample 5	27	31.9
Sample 6	24	31.8

[a]2θ is the angle between incident and diffracted X-ray.

Nanoparticles have a natural tendency to form aggregates and agglomerates due to attractive forces which become greater at the nanoscale and so the production of non-agglomerated nanoparticles is a challenging task.

Small crystalline particles with no defined geometry were also observed (Figure 3c) with a size distribution from 10 to 65 nm and a main value of 20 nm. These could be primary, non-aggregated particles.

EDS analysis, shown in Figure 4a, was also performed to verify purity of particles obtained by TEM analysis. Only lines for Cd, Si and O are observed.

The relative intensity of the Cd and Si lines in our case is significantly higher than those observed in studies[20,30] involving $CdSiO_3$ and Cd_2SiO_4, indicating a higher Cd/Si ratio corresponding to the phase Cd_3SiO_5. Moreover, this ratio increases steadily from $CdSiO_3$ to Cd_2SiO_4 to Cd_3SiO_5.

The SAED pattern (Figure 4b) consists mostly of regularly spaced spots of a single crystal, which can be indexed to the Cd_3SiO_5 X-ray diffraction based on the calculated interplanar spacing (d).[31] From the electron diffraction pattern, the spacing d can be obtained by equation 6:

$$\frac{1}{\text{reciprocal space}} = \text{interplanar spacing} \quad (6)$$

It is possible to compare these values to X-ray diffraction by Bragg's law (equation 7):

$$2d\text{sen}\theta = n\lambda \quad (7)$$

where λ is the X-ray wavelength (0.1542 nm), θ is given from diffractometry peak position and n is order of reflection, usually n = 1.

The calculated values are show in Table 2.

The nitrogen adsorption isotherm (Figure 5) can be identified as a type II by the IUPAC (International Union of Pure and Applied Chemistry) classification.[32] These results indicate a non-porous or macroporous adsorbent. However, the pore distribution indicates the presence of mesoporous with a diameter of 5 nm. This is expected due to the use of CTAB as a template.[33]

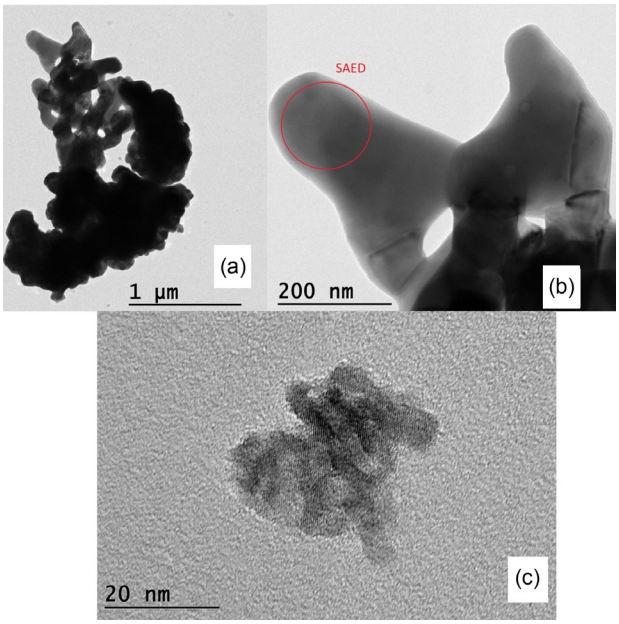

Figure 3. TEM images of sample 6 nanoparticles: (a) aggregated particles, (b) enlargement of a section to highlight particle coalescence and (c) primary particles observed.

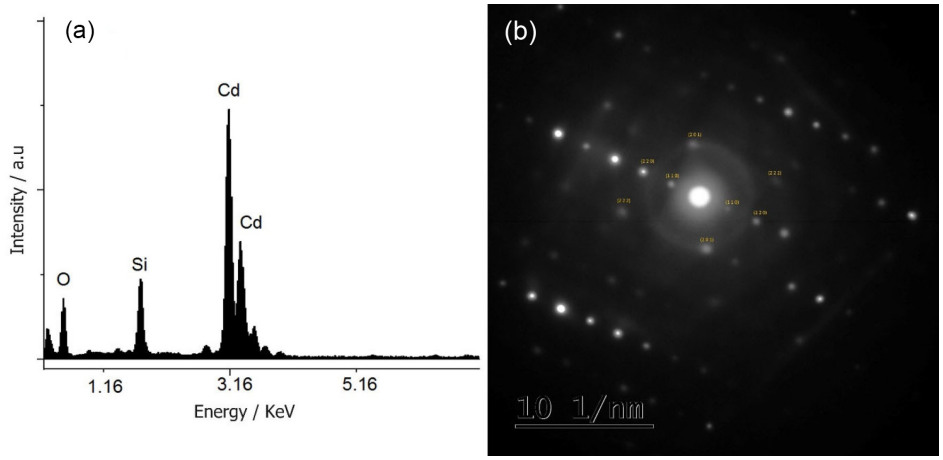

Figure 4. (a) EDS analysis and (b) SAED pattern of sample 6 nanoparticles.

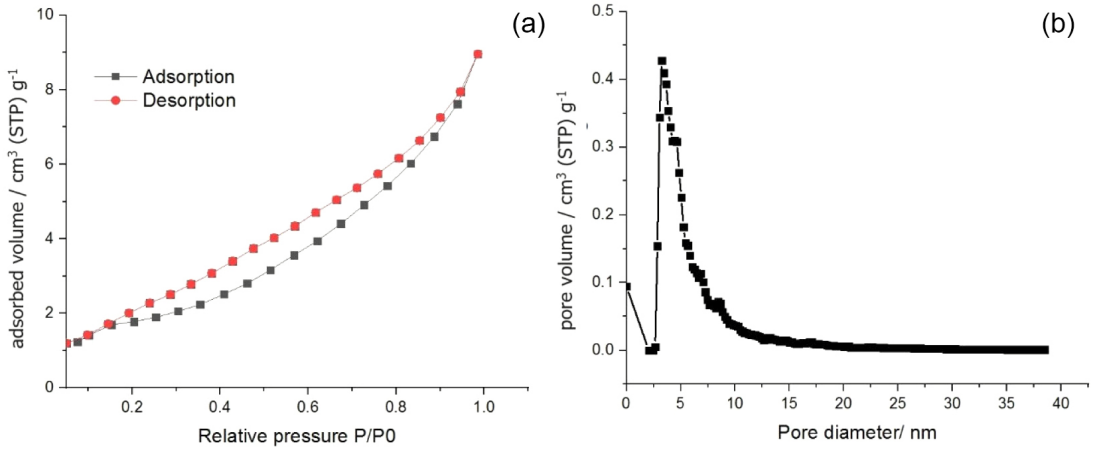

Figure 5. Nitrogen adsorption isotherm (a) and pore distribution (b) for sample 6.

Table 2. Calculated d spacing for sample 6 from XRD and SAED. JCPDS No. 00-026-0272 Cd_3SiO_5 is also shown for comparison

d XRD / nm	d SAED / nm	d JCPDS / nm	hkl
0.49	0.45	0.48	110
0.28	0.29	0.28	201
0.24	0.23	0.24	220
0.17	0.18	0.18	222

XRD: X-ray powder diffractometry; SAED: selected area electron diffraction; JCPDS: Joint Committee on Powder Diffraction Standards; d: interplanar spacing; hkl: Miller indices.

The desorption curve forms a hysteresis loop similar to a H3 type, that could be associated with non-rigid aggregates forming slit-like pores.[32]

The surface area was calculated by BET, DFT (density function theory) and BJH (Barret-Joyner-Halenda) methods. Table 3 shows these results. The values calculated are very similar, obtaining a surface area of 6-7 $m^2 g^{-1}$. The small values of surface area obtained could be associated to the presence of aggregates shown in Figure 3, since surface area depends on a combination of factors: size distribution, porosity and irregularities.

Table 3. Surface area calculated for sample 6

Sample 6	BET	DFT	BJH
Surface area / ($m^2 g^{-1}$)	6	7	6

BET: Brunauer-Emmett-Teller method; DFT: density function theory; BJH: Barret-Joyner-Halenda method.

Having obtained the material as a single phase, its luminescent and morphological properties can be studied in further detail.

Conclusions

Single-phase cadmium oxyorthosilicate Cd_3SiO_5 was successfully obtained for the first time using a sol-gel route applying pH 3 followed by heat treatment at 800 °C for 6 h. Phase purity was confirmed by X-ray diffraction as well as EDS and SAED analysis. TEM images reveal aggregates of nanoparticles, which are congruent with the surface area results and the synthetic method used. The surface area calculated by the BET method was 6 $m^2 g^{-1}$ with a pore diameter of 5 nm, indicating a material with mesopores.

Acknowledgments

The authors thank Conselho Nacional de Desenvolvimento Cientifico e Tecnológico (CNPq) process number 148039/2019-7, 162383/2023-1 and Fundação de Amparo à Pesquisa do Estado de São Paulo (FAPESP) process number 2011/19941-4 for financial support.

This study was financed in part by the Coordenação de Aperfeiçoamento de Pessoal de Nível Superior Brasil (CAPES), Finance Code 001.

References

1. Glasser, L. S. D.; Glasser, F. P.; *Inorg. Chem.* **1964**, *3*, 1228. [Crossref]
2. Hesse, K. F.; *Z. Kristallogr. - Cryst. Mater.* **1984**, *168*, 93. [Crossref]
3. Rojas-Hernandez, R. E.; Rubio-Marcos, F.; Rodriguez, M. A.; Fernandez, J. F.; *Renewable Sustainable Energy Rev.* **2018**, *81*, 2759. [Crossref]
4. Blasse, G.; Grabmayer, B. C.; *Luminescent Materials*, 1st ed.; Springer-Verlag: Berlin, 1994, ch. 1. [Link] accessed in July 2024
5. Basavara, R. B.; Nagabhushana, H.; Darshan, G. P.; Prasad, B. D.; Rahul, M.; Sharma, S. C.; Sudaramani, R.; Archana, K. V.; *Dyes Pigm.* **2017**, *147*, 364. [Crossref]

6. Su, M.; Liao, C.; Chen, D.; Shih, K.; Kong, L.; Tang, J.; Zhang, H.; Song, G.; *Waste Manage.* **2019**, *87*, 814. [Crossref]
7. Fowler, B. A.; *Toxicol. Appl. Pharmacol.* **2009**, *238*, 294. [Crossref]
8. Ono, K.; *J. Hazard. Mater.* **2013**, *262*, 741. [Crossref]
9. Hou, L.; Ji, S.; Zhang, Y.; Wu, X.; Zhang, L.; Liu, P.; *Front. Plant. Sci.* **2023**, *14*, 1. [Crossref]
10. Weil, M.; *Acta Crystallogr.* **2005**, *61*, 102. [Crossref]
11. Barbará, M. A. S. G.: *Um Estudo Estrutural e Óptico do Material Ortossilicato de Cádmio Dopado com Terras Raras*; MSc Dissertation, University of São Paulo, São Paulo, Brazil, 2018. [Link] accessed in July 2024
12. The Materials Project, *Cd_3SiO_5, mp-13820*, https://next-gen.materialsproject.org/materials/mp-13820, accessed in July 2024.
13. Glasser, L. S. D.; *Acta Crystallogr.* **1965**, *18*, 455. [Crossref]
14. Freire, E. B.; Santos, A. L. S.; Bispo, G. F. C.; Gomes, M. A.; Macedo, Z. S.; Jackson, R. A.; Valerio, E. M. G.; *J. Alloys Compd.* **2021**, *857*, 157580. [Crossref]
15. Santana, L. P.; de Almeida, E. S.; Soares, J.; Vichi, F. M.; *J. Braz. Chem. Soc.* **2011**, *22*, 2013. [Crossref]
16. Fonda, G. R.; *J. Phys. Chem.* **1939**, *46*, 561. [Crossref]
17. Abreu, C. M.: *Caracterização do Composto Luminescente $CdSiO_3$ Produzido por Rota Sol-Gel*; PhD Thesis, Universidade Federal de Sergipe, Sergipe, Brazil, 2014. [Link] accessed in July 2024
18. Santos, E. I. A. H.: *Síntese e Caracterização de Silicato de Cádmio Dopado com Íons de Metais de Transição e ou Terras Raras para Obtenção de Materiais com Luminescência Persistente*; MSc Dissertation, Universidade de São Paulo, São Paulo, Brazil, 2022. [Link] accessed in July 2024
19. Rodrigues, L. C. V.: *Preparação e Desenvolvimento do Mecanismo da Luminescência Persistente de Materiais Dopados com Íons Terras Raras*; PhD Thesis, Universidade de São Paulo, São Paulo, Brazil, 2012. [Link] accessed in July 2024
20. Masjedi-Arani, M.; Salavati-Niasari, M.; *Ultrason. Sonochem.* **2018**, *43*, 136. [Crossref]
21. Brinker, C.; Scherer, G.; *Sol-Gel Science: The Physics and Chemistry of Sol-Gel Processing*; 1st ed.; Academic Press: New York, 1990, ch. 3.
22. Esposito, S.; *Mater.* **2019**, *12*, 668. [Crossref]
23. Ristić, M.; Popović, S.; Musić, S.; *Mater. Lett.* **2004**, *58*, 2494. [Crossref]
24. Su, M.; Tang, J.; Liao, C.; Kong, L.; Xiao, T.; Shih, K.; Song, G.; Zhang, H.; *Environ. Pollut.* **2018**, *239*, 571. [Crossref]
25. Farias, D.; Abreu, C. M.; Novais, S. M. V.; Macedo, Z. S.; *J. Lumin.* **2018**, *194*, 535. [Crossref]
26. Abreu, C. M.; Silva, R. S.; *Sci. Plena* **2010**, *6*, 034801. [Link] accessed in July 2024
27. Rodrigues, L. C. V.; Brito, H. F.; Hölsä, J.; Lastusaari, M.; *Opt. Mater. Express* **2012**, *2*, 382. [Crossref]
28. Zhou, L.; Wang, X.; Ma, C.; Liu, S.; Ma, L.; Liu, J. J.; *J. Fuel Chem. Technol.* **2021**, *49*, 648. [Crossref]
29. Hincke, W. B.; *J. Am. Chem. Soc.* **1933**, *55*, 1751. [Crossref]
30. Manohar, B. M.; Nagabhushana, H.; Thyagarajan, K.; Prasad, B. D.; Prashantha, S. C.; Sharma, S. C.; Nagabhushana, B. M.; *J. Lumin.* **2015**, *161*, 247. [Crossref]
31. Luo, Z.; *Transmission Electron Microscopy Fundamentals*, vol. 1, 1st ed.; Momentum Press: New York, 2016, ch. 4.
32. Broekhoff, J. C. P.; *Stud. Surf. Sci. Catal.* **1979**, *3*, 663. [Crossref]
33. ALOthman, Z. A.; *Mater.* **2012**, *5*, 2875. [Crossref]

Submitted: February 09, 2024
Published online: July 15, 2024